Biophysical Journal, Volume 97

Supporting Material

Tryptophan Conformations Associated with Partial Unfolding in Ribonuclease T1

Samuel L. C. Moors, Abel Jonckheer, Marc De Maeyer, Yves Engelborghs, and Arnout Ceulemans

Supplementary material

Tryptophan Rotamers Reveal Partial Unfolding in Ribonuclease T1

Samuel L. C. Moors, Abel Jonckheer, Marc De Maeyer, Yves Engelborghs, and Arnout Ceulemans

METHODS

Molecular dynamics simulations

Molecular dynamics (MD) simulations were performed using the AMBER 2003 force field (1) with a modified version of the Amber 8 software (2). The smooth particle mesh Ewald method (3) was employed to accommodate long-range electrostatic forces. The nonbonded cutoff for van der Waals interactions was set to 8 Å. Covalent bonds involving hydrogen atoms were constrained using SHAKE (4). A time step of 1.5 fs was used. Samples were collected every 0.5 ps. The temperature was controlled using the weak-coupling algorithm (5). The initial structure was obtained from the X-ray structure of RNase T1 (PDB code 9RNT). Exact protonation states of the three histidine side chains were determined from their experimentally determined pKa values (6). At pH 6, all histidines are protonated. At pH 8, His^{27} is deprotonated at $N^{\delta 1}$, His^{40} and His^{92} are deprotonated at $N^{\varepsilon 2}$. Protonation states of the remaining titratable groups were determined using the H++ server (7) by means of a Poisson-Boltzmann continuum solvation model. The obtained protonation states for the remaining groups are identical to those of the free amino acids at pH 7. The charged proteins (-9 e at pH 8, -6 e at pH 6) were neutralized with sodium ions and solvated in a truncated octahedral box containing 4312 TIP3P (8) water molecules. The neutral solvated system was relaxed and equilibrated for 15 ns at 300 K. To improve sampling of the native state, the protein was allowed to move freely below 4.5 Å backbone root mean square deviation (bRMSD) from the X-ray structure. Above this threshold, the system was penalized by a harmonic restraint on the bRMSD with a force constant of 10 kcal mol^{-1} $Å^{-2}$. Solvent accessible surface areas (SASA) were calculated using the program VMD (9). Secondary structures were assigned with the program DSSPcont (10), which is a continuous version of the discrete classification used by the DSSP (11) program. Contacts are defined as occurring whenever the C^{α} atoms of two nonneighboring amino acids are within 6.5 Å of each other. The fraction of native contacts (Q) is taken as the fraction of contacts present in the X-ray structure, which contains 216 contacts. The bRMS fluctuation is defined as the bRMSD from the average structure after fitting the backbone atoms to the X-ray structure. H-bond energies were calculated with a modified Mayo potential (12,13), which treats salt bridges as a special case of (stronger) H-bonds.

Estimation of statistical significance

The statistical uncertainties of thermodynamic averages were calculated using the statistical inefficiency method (14). Given an observable *A*, the uncertainty in the average $\overline{A}$ is calculated as

$$\sigma^2(\overline{A}) = \frac{s\sigma^2(A)}{m}, \qquad \text{(S1)}$$

where $\sigma^2(A)$ is variance of *A*, *s* denotes the statistical inefficiency, and *m* is the number of data points. The statistical inefficiency is determined by block averaging. We plot $m_b\sigma^2(\overline{A_b})/\sigma^2(A)$ as a function of m_b, where m_b is the number of data points in each block

b and A_b is the average of block b. The value of s is asymptotically approached with increasing block size (see Fig. S5)

$$s = \lim_{m_b \to \infty} \frac{m_b \sigma^2(\overline{A_b})}{\sigma^2(A)}. \quad \text{(S2)}$$

Figure S1

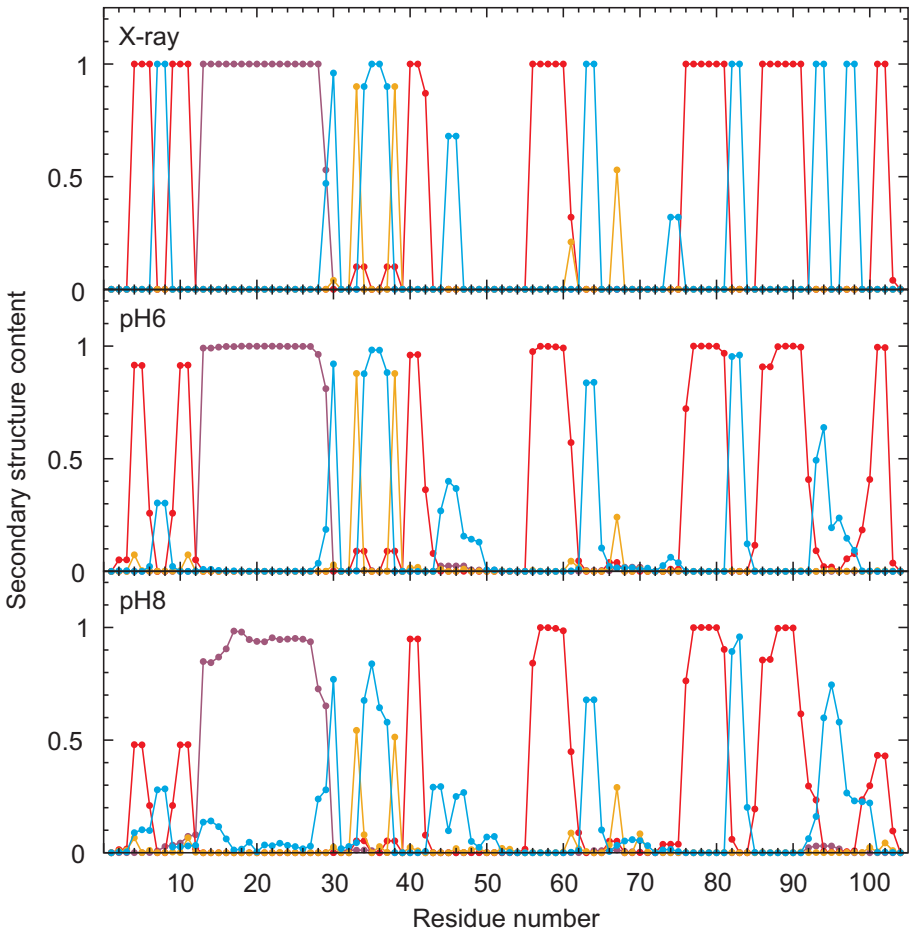

Secondary structure content as a function of residue number for the X-ray structure and the simulations corresponding to pH 6 and pH 8. Color codes are: α-helix (purple), β-sheet (red), β-bridge (orange), hydrogen bonded 3, 4 or 5 turn (cyan) as defined in the DSSPcont program (10). A β-bridge is assigned between residues *i* and *j* if there are two H-bonds characteristic of β-structure.

Figure S2

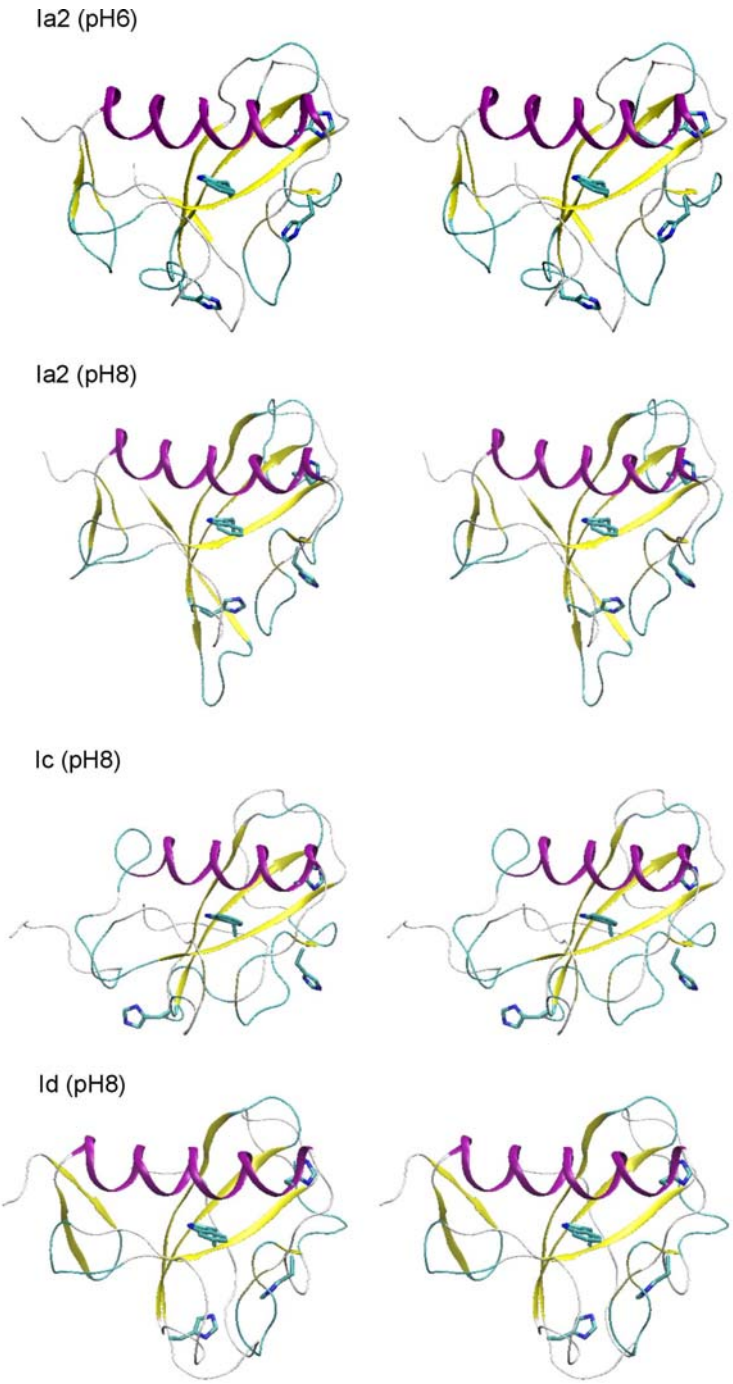

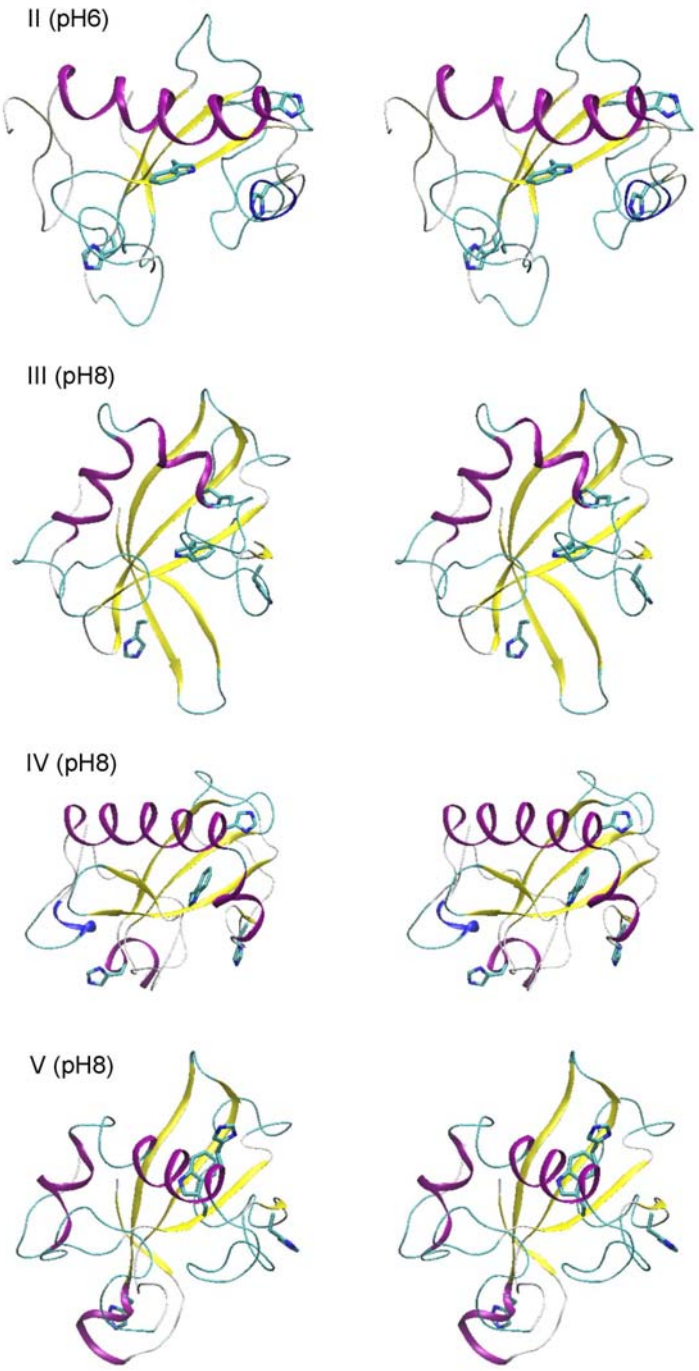

Stereofigures for representative RNase T1 conformations of the most stable substates and alternative Trp^{59} rotamers at pH 6 and 8, supplementing Fig. 5.

Figure S3

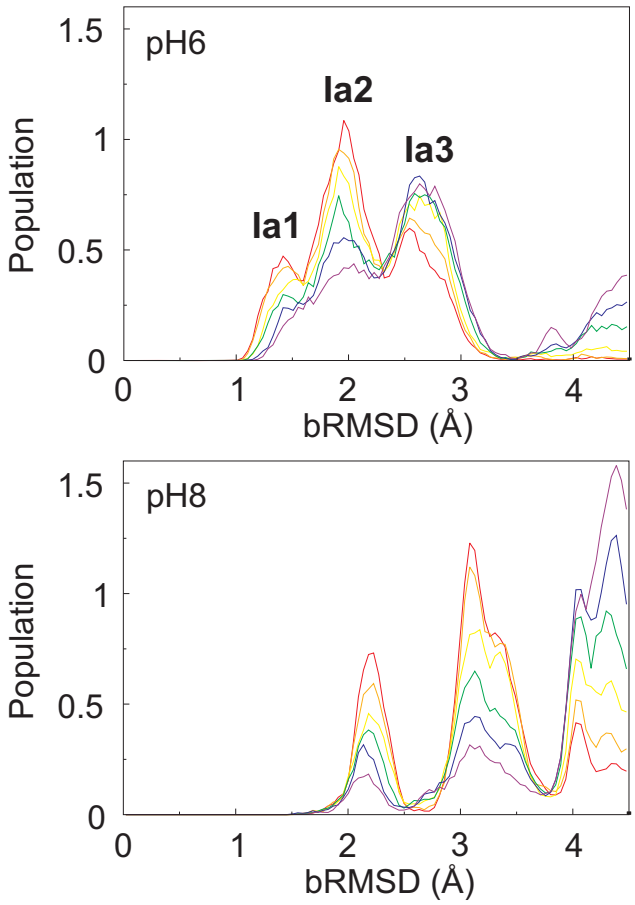

Normalized populations of the backbone RMSD from the X-ray structure for the simulations at pH 6 and pH 8 and at different temperatures. Color codes are: 300 K (red), 305.9 K (orange), 312 K (yellow), 318.2 K (green), 324.5 K, (blue), 330.9 K (violet).

Figure S4

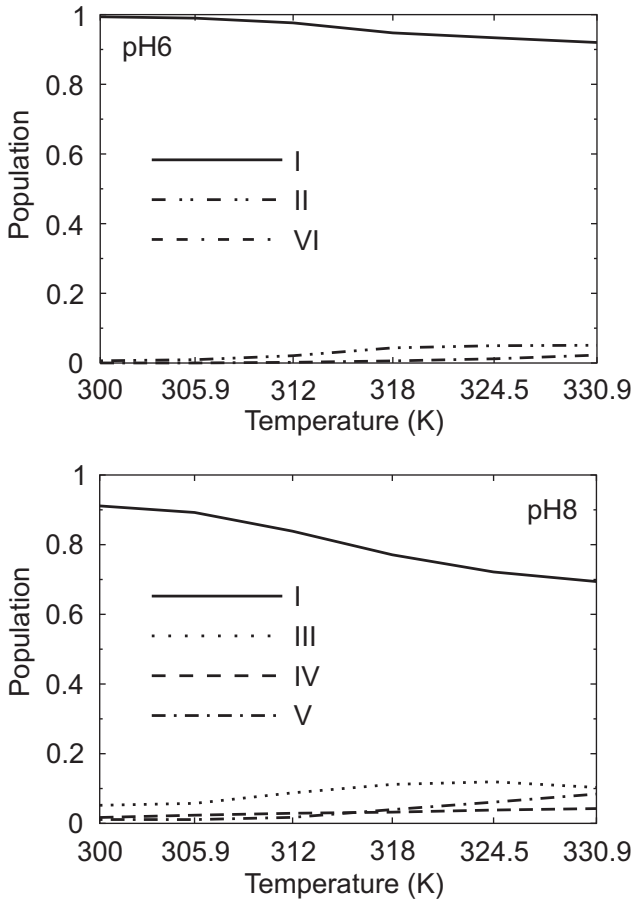

Rotamer populations as a function of temperature for the REM simulations at pH 6 and pH 8 with numbering according to Fig. 7.

Figure S5

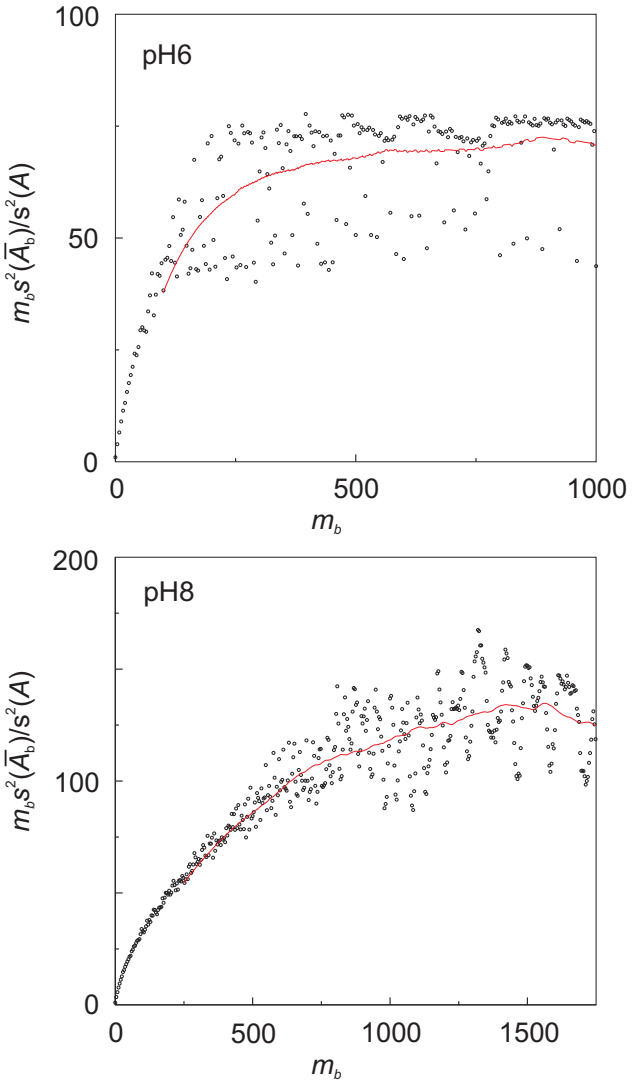

Determination of the statistical inefficiency for the major rotamer I at pH 6 and pH 8, using the statistical inefficiency method. The red line denotes a running average.

Figure S6

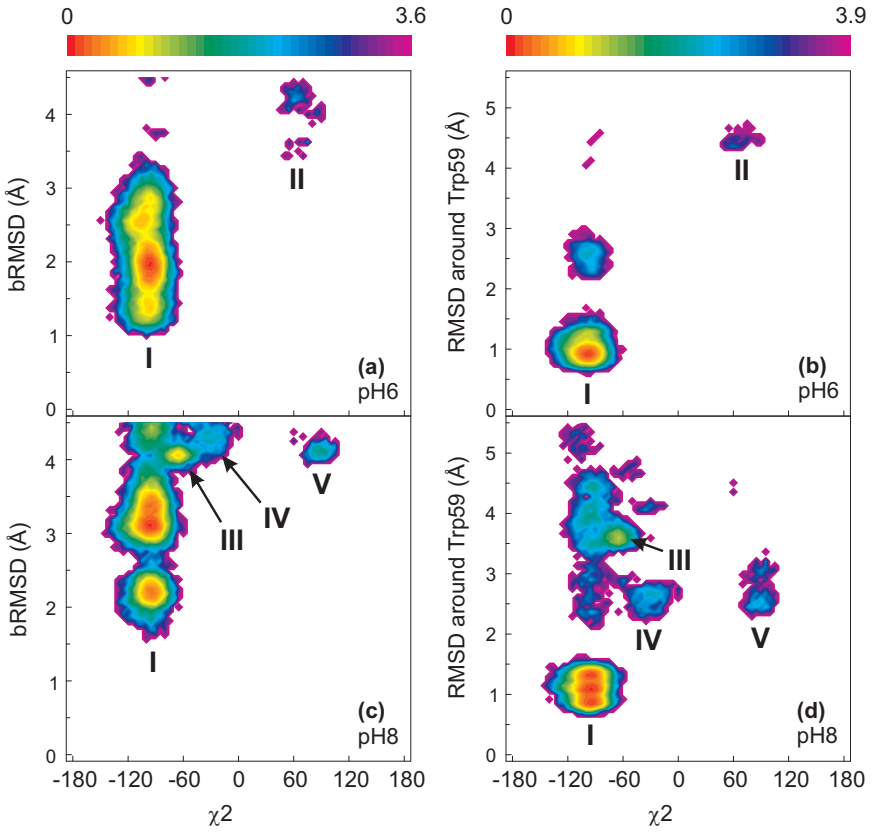

Free energy as a function of Trp^{59} χ2 and **(a,c)** bRMSD from the X-ray structure, **(b,d)** total RMSD from the X-ray structure for all residues within a sphere of 4.5 Å around Trp^{59} in the X-ray structure (numbering according to Fig. 7).

Table S7

Histidine H-bond energies

H-bond	*E* (kcal mol^{-1}) pH 6	pH 8
His^{27} N$^{\varepsilon 2}$-H$^{\varepsilon 2}$ -- Glu^{82} O$^{\varepsilon 1/\varepsilon 2*}$	-2.97	-0.32
Total His^{27†}	**-2.97**	**-0.32**
His^{40} N$^{\delta 1}$-H$^{\delta 1}$ -- Asn^{36} O*	-0.25	-0.23
His^{40} N$^{\delta 1}$-H$^{\delta 1}$ -- Ser^{37} O*	-0.66	-0.41
His^{40} N$^{\delta 1}$-H$^{\delta 1}$ -- Lys^{41} O	-0.21	-0.12
His^{40} N$^{\delta 1}$-H$^{\delta 1}$ -- Glu^{58} O$^{\varepsilon 1/\varepsilon 2}$	-2.18	-1.71
His^{40} N$^{\varepsilon 2}$-H$^{\varepsilon 2}$ -- Asn^{36} O	-0.41	
His^{40} N$^{\varepsilon 2}$-H$^{\varepsilon 2}$ -- Asn^{36} O$^{\delta 1}$	-0.26	
His^{40} N$^{\varepsilon 2}$-H$^{\varepsilon 2}$ -- Glu^{58} O$^{\varepsilon 1/\varepsilon 2*}$	-5.14	
Total His^{40†}	**-9.11**	**-2.47**
His^{92} N$^{\delta 1}$-H$^{\delta 1}$ -- Ala^{75} O	-0.22	-0.09
His^{92} N$^{\delta 1}$-H$^{\delta 1}$ -- Asp^{76} O$^{\delta 1/\delta 2}$	-0.56	-0.97
His^{92} N$^{\delta 1}$-H$^{\delta 1}$ -- Thr^{93} O	-0.42	-0.43
His^{92} N$^{\delta 1}$-H$^{\delta 1}$ -- Ser^{96} O	-0.00	-0.15
His^{92} N$^{\delta 1}$-H$^{\delta 1}$ -- Gly^{97} O	-0.02	-0.42
His^{92} N$^{\delta 1}$-H$^{\delta 1}$ -- Asn^{99} O*	-0.60	-0.05
His^{92} N$^{\varepsilon 2}$-H$^{\varepsilon 2}$ -- Ser^{8} OG	-0.33	
His^{92} N$^{\varepsilon 2}$-H$^{\varepsilon 2}$ -- Asp^{76} O$^{\delta 1/\delta 2}$	-0.26	
His^{92} N$^{\varepsilon 2}$-H$^{\varepsilon 2}$ -- Gly^{97} O	-0.95	
His^{92} N$^{\varepsilon 2}$-H$^{\varepsilon 2}$ -- Asn^{98} O	-0.05	
His^{92} N$^{\varepsilon 2}$ -- Arg^{77} N$^{\eta 1/2}$-H$^{\eta 11/12/21/22}$		-0.31
Total His^{92†}	**-3.41**	**-2.42**

*H-bonds present in the X-ray structure.
†Sum of all H-bond energies connected with the His side chain.

REFERENCES

1. Duan, Y., C. Wu, S. Chowdhury, M. C. Lee, G. M. Xiong, W. Zhang, R. Yang, P. Cieplak, R. Luo, T. Lee, J. Caldwell, J. M. Wang, and P. Kollman. 2003. A point-charge force field for molecular mechanics simulations of proteins based on condensed-phase quantum mechanical calculations. *Journal of Computational Chemistry* 24:1999-2012.
2. Case, D. A., T. A. Darden, T. E. Cheatham III, C. L. Simmerling, J. Wang, R. E. Duke, R. Luo, K. M. Merz, B. Wang, D. A. Pearlman, M. Crowley, S. Brozell, V. Tsui, H. Gohlke, J. Mongan, V. Hornak, G. Cui, P. Beroza, C. Schafmeister, J. W. Caldwell, W. S. Ross, and P. A. Kollman. 2004. AMBER 8. University of California, San Francisco.
3. Essmann, U., L. Perera, M. L. Berkowitz, T. Darden, H. Lee, and L. G. Pedersen. 1995. A Smooth Particle Mesh Ewald Method. *Journal of Chemical Physics* 103:8577-8593.
4. Ryckaert, J.-P., G. Ciccotti, and H. J. C. Berendsen. 1977. Numerical integration of the cartesian equations of motion of a system with constraints: Molecular dynamics of n-alkanes. *Journal of Computational Physics* 23:327-341.
5. Berendsen, H. J. C., J. P. M. Postma, W. F. Vangunsteren, A. Dinola, and J. R. Haak. 1984. Molecular-Dynamics with Coupling to an External Bath. *Journal of Chemical Physics* 81:3684-3690.
6. Spitzner, N., F. Lohr, S. Pfeiffer, A. Koumanov, A. Karshikoff, and H. Ruterjans. 2001. Ionization properties of titratable groups in ribonuclease T-1 - I. pK(a) values in the native state determined by two-dimensional heteronuclear NMR spectroscopy. *European Biophysics Journal with Biophysics Letters* 30:186-197.
7. Gordon, J. C., J. B. Myers, T. Folta, V. Shoja, L. S. Heath, and A. Onufriev. 2005. H++: a server for estimating pK(a)s and adding missing hydrogens to macromolecules. *Nucleic Acids Research* 33:W368-W371.
8. Jorgensen, W. L., J. Chandrasekhar, J. D. Madura, R. W. Impey, and M. L. Klein. 1983. Comparison of Simple Potential Functions for Simulating Liquid Water. *Journal of Chemical Physics* 79:926-935.
9. Humphrey, W., A. Dalke, and K. Schulten. 1996. VMD: Visual molecular dynamics. *Journal of Molecular Graphics* 14:33-&.
10. Carter, P., C. A. F. Andersen, and B. Rost. 2003. DSSPcont: continuous secondary structure assignments for proteins. *Nucleic Acids Research* 31:3293-3295.
11. Kabsch, W., and C. Sander. 1983. Dictionary of Protein Secondary Structure - Pattern-Recognition of Hydrogen-Bonded and Geometrical Features. *Biopolymers* 22:2577-2637.
12. Dahiyat, B. I., D. B. Gordon, and S. L. Mayo. 1997. Automated design of the surface positions of protein helices. *Protein Science* 6:1333-1337.
13. Rader, A. J., B. M. Hespenheide, L. A. Kuhn, and M. F. Thorpe. 2002. Protein unfolding: Rigidity lost. *Proceedings of the National Academy of Sciences of the United States of America* 99:3540-3545.
14. Allen, M. P., and D. J. Tildesley. 1987. Computer Simulation of Liquids. Oxford University Press, New York.